

available at [www.sciencedirect.com](http://www.sciencedirect.com)journal homepage: [www.elsevier.com/locate/carbon](http://www.elsevier.com/locate/carbon)

# The effect of experimental parameters on the synthesis of carbon nanotube/nanofiber supported platinum by polyol processing techniques

Seth L. Knupp, Wenzhen Li, Odysseas Paschos, Thomas M. Murray, Jeremy Snyder, Pradeep Haldar\*

Energy and Environmental Technology Applications Center (E2TAC), College of Nanoscale Science and Engineering (CNSE), University at Albany, State University of New York, 255 Fuller Road, Albany, NY 12203, USA

## ARTICLE INFO

### Article history:

Received 29 January 2008

Accepted 1 May 2008

Available online 15 May 2008

## ABSTRACT

Developing corrosion resistant carbon nanotube (CNT) and carbon nanofiber (CNF) supported Pt catalysts with optimized particle size is important for proton exchange membrane fuel cells. We investigated the effects of deposition technique (conventional refluxing and microwave irradiation), water content, carbon support and metal loading on the average Pt particle size and electrochemically active surface area (ECSA). BET surface area measurements, Fourier transform infrared spectroscopy, X-ray diffraction, thermal gravimetric analysis, transmission electron microscopy and cyclic voltammetry were used to characterize all the CNT/CNF supported catalysts. Processing was accelerated via microwave irradiation without significantly affecting Pt particle size as compared to conventional refluxing especially for high surface area CNT supported low Pt loading (10 wt%) catalyst. Adjusting the water content during synthesis effectively controlled the Pt particle size and size distribution regardless of the heating method, carbon support and metal loading. The ECSA of the samples was found to be dependent on Pt particle size which further depends on the water content during synthesis, support surface area and Pt loading. Optimization of deposition conditions leads to higher ECSA than seen in a commercially available carbon black supported catalyst.

© 2008 Elsevier Ltd. All rights reserved.

## 1. Introduction

Proton exchange membrane fuel cells (PEMFCs) are receiving much attention today due to their unique properties and their ability to create an efficient and clean source of energy [1]. However, the high cost of electrocatalysts, e.g. Pt and degradation of stack voltage are the two main factors hampering their commercialization. The last two decades witnessed a 10 time reduction in membrane electrode assembly (MEA) Pt loading from ca. 4 to 0.4 mg/cm<sup>2</sup>. At the anode, fast kinetics of hydrogen oxidation have made it possible to achieve low

loadings (0.05 mg/cm<sup>2</sup>) compared to conventional loadings (0.2 mg/cm<sup>2</sup>) without any fuel cell performance reduction [2]. However, at the cathode, reducing Pt loading is more challenging. The oxygen reduction reaction (ORR) is a highly irreversible reaction. The kinetics of the cathodic reaction are much slower than at the anode and still, there is not a clear mechanism to explain this. A recent study based on density functional theory suggests the origin of high overpotential for the ORR may come from stable intermediates – adsorbed oxygen and hydroxyl species at potentials close to equilibrium slows kinetics for activated proton and electron transfer

\* Corresponding author. Fax: +1 518 437 8687.

E-mail address: [phaldar@uamail.albany.edu](mailto:phaldar@uamail.albany.edu) (P. Haldar).

0008-6223/\$ - see front matter © 2008 Elsevier Ltd. All rights reserved.

doi:10.1016/j.carbon.2008.05.007

processes [3]. A further reduction in Pt loading to ca. 1/4 of the current state-of-the-art MEA cathode catalyst layer, from about 0.4 to 0.1 mg/cm<sup>2</sup> without any loss in cell voltage, is needed in order to achieve widespread commercial application of PEMFCs [4].

Utilizing high surface area carbon nanomaterials like carbon nanotubes (CNTs) and carbon nanofibers (CNFs) is expected to improve Pt activity as well as employ their impressive electrical, mechanical and structural properties [5]. It has been reported that the use of CNT/CNF supported catalysts has shown higher ORR activity compared to conventional carbon black supported Pt catalysts [6–13] and has the potential to reduce cathode Pt loading of a MEA. Matsumoto et al. [7] found that a 12 wt% Pt deposited CNT electrode provides 10% higher voltage than 29 wt% Pt deposited on carbon black and reduces Pt usage by 60% in PEMFCs when using hydrogen and oxygen. Yuan et al. [9] have further shown that CNFs were able to give better performance compared to CNTs.

Another major challenge is degradation of fuel cell voltage with time, caused by loss of Pt surface area resulting from oxidation of the carbon support. Wang et al. [14] have shown that multiwalled CNTs can be more durable and can outlast the lifetime of conventional Vulcan XC72. An additional benefit for CNT/CNF as electrocatalyst support is their potential to improve mass transport [10,11]. This is because a CNT/CNF based catalyst electrode allows fuel and oxidant access to the densely scattered triple phase boundaries more effectively.

Catalyst synthesis techniques strongly determine the metal nanoparticle size, distribution and dispersion on carbon support, thus ultimately controlling their catalytic activity and durability. Li et al. [6,8] reported a simple polyol glycol method for preparing size selected and uniformly dispersed Pt nanoparticles via conventional reflux oil bath heating. An alternative method involves microwave irradiation. This allows a substance to uniformly heat through a glass reaction vessel, which leads to more homogenous nucleation and shorter crystallization time compared to conventional heating methods [15–18]. A sonochemical technique was described by Xing et al. [19] which involved refluxing multiwalled CNTs in a nitric and sulfuric acid mixture to generate surface functional groups in order to attract Pt ions during deposition. This technique is used to oxidize the walls of the nanotubes while breaking bonds and leaving behind negatively charged functional groups. Carboxylic, carbonyl and hydroxyl functional bonds were found to be present and identified using FTIR. Systematic comparison of different synthesis parameters such as carbon support, Pt loading, water content and heating method have not yet been well elucidated.

While previous studies have shown the effectiveness of using CNT and CNF as catalyst supports, the focus of this study was to optimize the deposition of catalyst on those supports. We examined the effects of synthesis technique, carbon support, platinum loading and water content on the Pt particle size and size distribution. Conventional oil bath heating was compared to an alternative technique, microwave irradiation, using the polyol process. The method works on a mechanism described by Bock et al. [20] in which ethylene glycol (EG) acts as a reducing agent to Pt precursor (K<sub>2</sub>PtCl<sub>4</sub>)

by supplying electrons to the reaction. Parameters that were investigated included heating method, catalyst metal loading and water content in the synthesis system and their effects were shown on two different diameter carbon materials including CNTs and CNFs. Characterization methods that were employed to analyze the CNT and CNF supported Pt catalysts included thermal gravimetric analysis (TGA) to determine Pt metal loading, X-ray diffraction (XRD) to measure average Pt particle size, transmission electron microscopy (TEM) to determine Pt particle size and size distribution and cyclic voltammetry (CV) to obtain information about their ECSA.

## 2. Experimental

Research grade (purity > 95%) bamboo structured multiwalled carbon nanotubes were purchased from NanoLab Inc. (diameter 30 ± 10 nm, length 1–5 μm) and carbon nanofibers (Pyrograf-III PR-19HHT) were purchased from Applied Science Inc. (diameter 150 ± 50 nm, length: 30–100 μm). Potassium tetrachloroplatinate (K<sub>2</sub>PtCl<sub>4</sub>) was obtained from STREM Chemicals, Inc. and was diluted with deionized water to form a homogenous 0.01 M solution.

Oxidation of both CNTs and CNFs was done using the method described by Xing et al. [19]. Both carbon supports were exposed to a highly concentrated nitric and sulfuric acid mixture at 60 °C. The mixture was sonicated to enhance uniformity of functionalization and remove any amorphous carbon. Various treating periods (1 h, 2 h, 3 h, 4 h) were evaluated to determine the optimum functionalization time. The solution was then diluted with deionized water and centrifuged using an Eppendorf 5804 at 10,000 RPM for 5 min cycles until the pH was 7. After neutralization, the carbon nanomaterial was dried in air at 100 °C.

For analysis of surface vibrational bonds a Nicolet Magna-IR 750 Spectrometer Series II Fourier transform infrared (FTIR) spectrometer was used. Functionalized CNTs or CNFs were mixed with potassium bromide until a uniform grey powder was formed. The sample was loaded into the Thermo Spectra-Tech 007-172 powder holder.

The oxidized carbon nanomaterial (CNT and CNF) powder was used as catalyst support for all catalysis reported below. In both methods (conventional refluxing and microwave irradiation), EG–water mixture was used as a medium to disperse the powder in solution and was sonicated until all agglomerates were broken and dispersed evenly. The appropriate amount of precursor was then added drop wise and the solution was sonicated again to assure that the precursor ions would scatter throughout the solution and disperse evenly. For conventional reflux heating method, the solution was heated at 125 °C for 2 h using an oil bath, under refluxing conditions and agitation. In the case of microwave irradiation method, the solution was heated in a domestic microwave oven. Heating cycles were done at 700 W for 15 s on and 60 s off and repeated for 30 min. Vacuum filtration was used with the aid of 80 °C deionized water to help dissolve excess chloride ions and wash away the EG. Platinized samples were dried at 100 °C in a nitrogen environment. Investigation of the dependency of particle size and distribution was done by varying water content in the EG–water mixture and

catalyst metal loading. Samples were prepared with 10 wt% and 30 wt% Pt supported on CNTs and CNFs and water content was altered during synthesis from 10 to 30 vol%. The CNT/CNF catalysts were given names such as, “MCNF30Pt10DI”, “CCNT10Pt30DI”, where ‘M’ and ‘C’ denote ‘microwave’ and ‘conventional’ heating, ‘CNF’ and ‘CNT’ mean ‘carbon nanofibers’ and ‘carbon nanotubes’, the first number ‘30’ or ‘10’ mean the catalyst loading was ‘30 wt%’ or ‘10 wt%’, and the second number ‘10’ or ‘30’ mean ‘10 vol%’ or ‘30 vol%’ DI water in the EG–water mixture.

All samples were analyzed by TGA and XRD in order to confirm Pt loading, crystalline structure and particle size. TGA was performed with a TA Instruments thermo gravimetric analyzer (TGA 2050). By heating compressed air at 5 °C/min from room temperature to 1000 °C, carbon is gradually oxidized leaving behind unsupported Pt. XRD patterns were recorded on an X-ray diffractometer from SCINTAG Inc. (XDS 2000) using  $\text{CuK}\alpha$  radiation. The average Pt particle size was calculated based on the Pt(220) diffraction peak. The CNT/CNF supported catalysts were also characterized using a high resolution Field Emission Electron Microscope (JEOL JEM2010F) operating at 200 kV to obtain information about Pt particle size, size distribution and Pt dispersion on carbon supports.

A conventional three electrode cell was used for CV experiments where a Ag wire was used as a reference electrode (−0.362 vs. RHE), a Pt screen was used as a counter electrode and the catalyst dispersed on a glassy carbon (GC) electrode (area: 0.1926  $\text{cm}^2$ ) was used as a working electrode. CV curves were obtained using a potentiostat instrument (PARSTA 2273). The catalyst thin layer on the GC electrode had a fixed loading of 26  $\mu\text{g}/\text{cm}^2$ . In order to promote adhesion, 10  $\mu\text{L}$  of 0.05 wt% Nafion solution was added drop wise to the active catalyst layer. A 0.5M  $\text{H}_2\text{SO}_4$  solution was used as electrolyte and was heated and held at 60 °C during the experiment for simulating a fuel cell operating temperature. CV measurements were obtained after high purity nitrogen

purged the electrolyte solution for 20 min. The scan rate was 50 mV/s and scan range was from −0.3542 V to 0.9669 V (vs. Ag wire). A commercial Pt/CB catalyst (20 wt%) with the same GC loading was also tested as a reference sample.

### 3. Results and discussion

Fig. 1 illustrates the mechanism of the polyol process in which the carbon nanomaterial is first exposed to an oxidative environment, leaving behind negatively charged groups. The  $\text{Pt}^{2+}$  ions then diffuse to these functional sites via electrostatic attraction to form nucleation sites. Heating throughout the reaction causes the ethylene glycol to be oxidized to form oxalic acid and glycolic acid yielding sufficient electrons to reduce the  $\text{Pt}^{2+}$  ions to the  $\text{Pt}^0$  oxidation state [20,21]. The metallic Pt grains are thereby formed and further agglomerated to form nanoparticles.

FTIR was used to study the surface functionalization of the oxidized CNTs. Fig. 2 presents a spectrum of pristine CNTs that is compared to the 1, 2, 3 and 4 h exposure to  $\text{HNO}_3$  and  $\text{H}_2\text{SO}_4$  reagents. The peaks at 1000–1100  $\text{cm}^{-1}$  can be attributed to C–O symmetrical stretching, at 1401  $\text{cm}^{-1}$  O–H bending occurs, at 2853–3000  $\text{cm}^{-1}$  C–H stretching and at 3600–3700  $\text{cm}^{-1}$  O–H stretching [22–26]. Comparing the FTIR spectra, an amplified signal in intensity is revealed for an increasing time of exposure to the acid for all of the identifiable peaks present. In addition, it shows three hours of exposure to the aggressive reagents was sufficient time to treat the carbon material and to obtain ample surface modifications.

A representative TGA plot is shown in Fig. 3, in which the temperature is ramped from 25 to 1000 °C at 5 °C/min. CNFs begin oxidizing at  $\sim 300$  °C and are completely exhausted at 700 °C. The final sample weight is around 13% and 32% for 10 wt% and 30 wt% Pt/CNFs catalysts (MCNF10Pt10DI, MCNF30Pt10DI) respectively. The deviation between calculated and measured loadings may be due to presence of trace

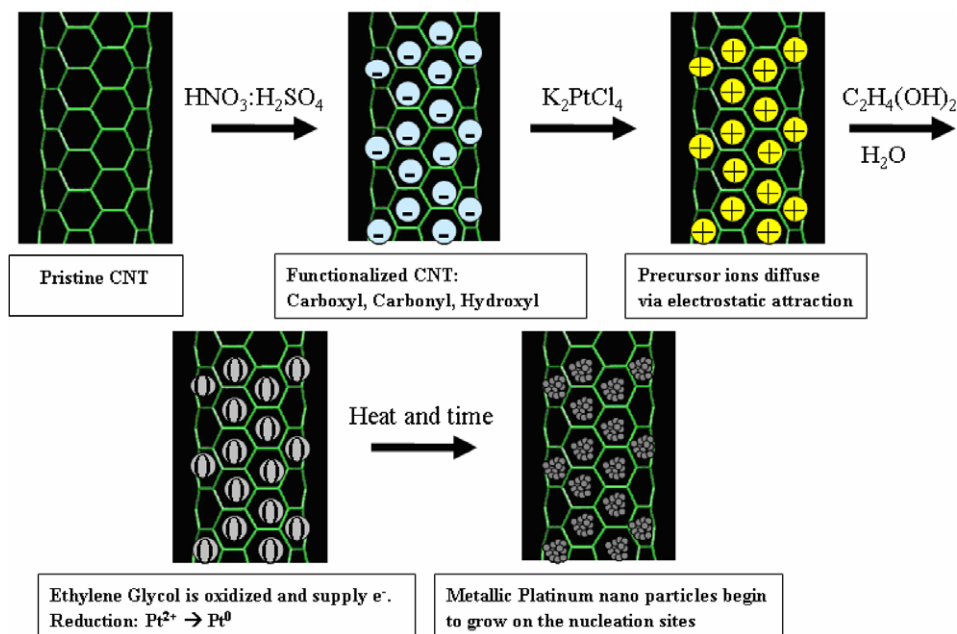
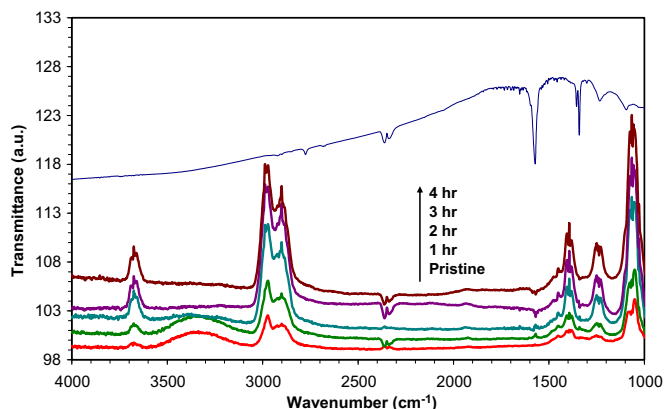
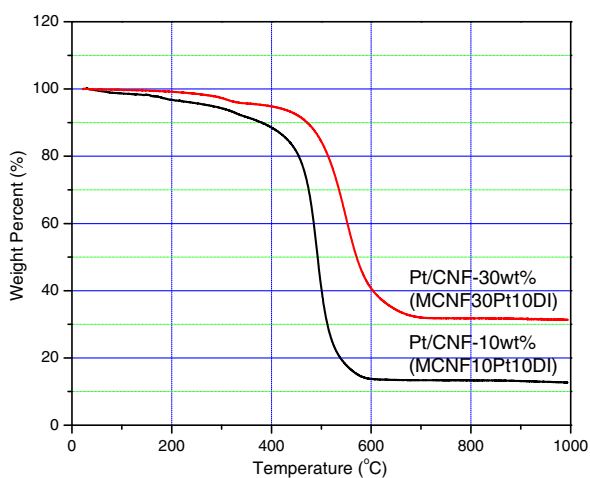


Fig. 1 – Schematic representation of the working mechanism behind the polyol synthesis method.



**Fig. 2 – Fourier transform Infrared spectrum (FTIR) on functionalized carbon nanotubes (1000–1100  $\text{cm}^{-1}$  C–O symmetrical stretching, 1200–1300  $\text{cm}^{-1}$  C–O asymmetrical stretching, 1401  $\text{cm}^{-1}$  O–H bending, 2853–3000  $\text{cm}^{-1}$  C–H stretching, 3600–3700  $\text{cm}^{-1}$  O–H stretching).**



**Fig. 3 – TGA of the 10 wt% and 30 wt% Pt/CNF.**

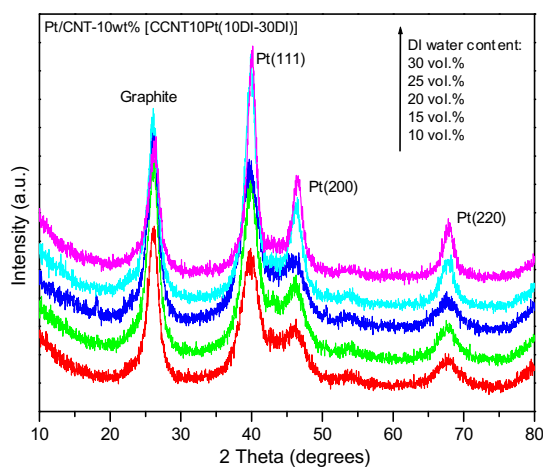


**Fig. 4 – XRD patterns of the Pt/CNT catalyst (10 wt%), prepared by conventional heating, DI water: 10, 15, 20, 25, 30 vol%).**

residues such as Fe or Co metals during chemical vapor deposition growth process of the CNF. Also Pt can be oxidized causing a deviation in weight percent.

Representative XRD spectra for 10 wt% Pt supported CNT catalysts prepared by conventional refluxing heating are shown in Fig. 4. The catalyst samples are prepared using different water content ranging from 10 vol% to 30 vol% in the synthesis system. XRD spectra of the catalysts show the standard Pt peaks at 39.8° Pt(111), 46.2° Pt(200), and 67.6° Pt(220). Since Pt(220) diffraction peak is isolated from all the others, it was used to measure the average particle size of the nanoparticles by means of the Scherrer formula

$$L = \frac{0.9 \times \lambda}{B \times \theta}$$

where  $L$  is the average particle size,  $\lambda$  is the sources wavelength,  $B$  is the full width at half maximum of the peak position and  $\theta$  is the angle at which the diffraction peak arises.

Fig. 5 shows XRD spectra on the Pt(220) peak for the 10 wt% CNT prepared by conventional heating. The size of Pt nanoparticles was calculated to be 2.3 nm for 10 vol%,

3.1 nm for 15 vol%, 3.3 nm for 20 vol%, 3.9 nm for 25 vol% and 5.0 nm for 30 vol%.

This indicates there is a trend of an increase in Pt particle size with increasing water to EG ratio.

The average Pt particle size of all nanocarbon supported Pt samples (different carbon support, loading, synthesis method) versus water content (vol%) is plotted in Fig. 6. It has been reported based on a similar reflux heating process that with increasing water content in the synthesis system, the Pt particle size gets larger [6,8].

Here we show a universal rule for controlling particle size for all samples regardless of heating method, carbon support and metal loading by simply adjusting the water content during synthesis. Pt nucleation and particle size growth are two key processes to control Pt nanoparticle size. If we can effectively separate the two processes, we can obtain monodispersed metal nanoparticles [27]. During synthesis, high viscosity EG can effectively stabilize the diffusion of Pt nanoparticles to aggregate to larger particles. EG has a steric

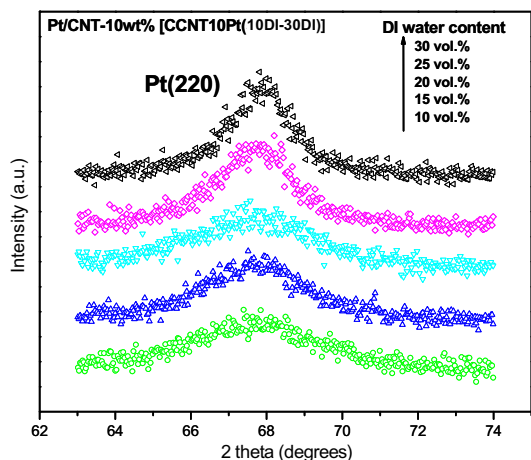


**Fig. 5 – XRD patterns of the Pt(220) diffraction peak for the Pt/CNT catalyst (10 wt%, prepared by conventional heating, DI water: 10, 15, 20, 25, 30 vol%).**

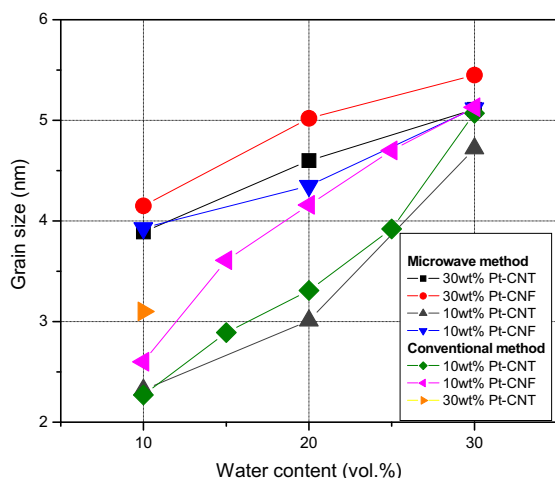


**Fig. 6 – Average Pt particle size versus water content.**

hindrance effect preventing Pt agglomeration. As water content is increased during synthesis these protective effects are reduced, thus larger average Pt particles are synthesized. In addition, the boiling point of EG–water mixture reduces with decreasing EG concentration, e.g. 135 °C for 10 vol% water, while ca. 110 °C for 30 vol% water. The low reaction temperature may be too low to completely initiate the nucleation reaction and as a result, grain growth is kinetically more favorable [18]. The lower temperature hinders sharp separation between metal nuclei formation and metal nanoparticle growth processes, which is generally believed to be a dominant factor for synthesis of small nanoparticles with narrow size distribution [28]. Other observed trends are as follows:

(1) Synthesis method effect – Conventional reflux method and microwave irradiation method (10 vol% water and 10 wt% Pt loading), were both able to produce similar results (~2.3 nm Pt particles) without using sodium hydroxide as a pH adjuster. When metal loading

increased from 10 wt% to 30 wt%, the Pt particle size was larger for microwave prepared samples, e.g., 3.1 nm for CCNT30Pt10DI and 3.9 nm for MCNT30Pt10DI. This is probably because heating a high ratio of Pt precursor to nanocarbon support quickly and unevenly results in larger particle sizes and wider size distribution, as compared to heating uniformly and slowly in the conventional reflux method. Modification of our microwave reactor to include a condenser, gas delivery system and agitation will ensure a more homogeneous deposition. This work is underway in our lab.

(2) Pt metal loading effect – It is widely accepted that higher metal loading needs a catalyst support with high surface area [29]. If the surface area is fixed, the high loading catalyst has a larger average particle size. This trend is also shown in our work. As the loading of Pt is increased, agglomeration is more rampant and larger particles begin to form, therefore the average Pt particle size gets larger.

(3) Carbon support effect – CNFs used in this paper had a diameter of 100–200 nm, which is larger than the CNTs (20–40 nm). BET experiments were performed to obtain information about surface area of the carbon supports. CNFs had a smaller surface area (67 m<sup>2</sup>/g) compared to CNTs (270 m<sup>2</sup>/g). Therefore it is consistent with our expectation that the larger diameter CNF produced larger nanoparticles than those produced on CNT under the same synthesis conditions. This trend is clearly shown in Fig. 6. For example, using 10 vol% water, 10 wt% Pt, in the microwave irradiation method, the average Pt particle size for MCNT10Pt10DI is 2.3 nm, which was smaller than that for MCNF10Pt10DI (3.9 nm).

Representative TEM micrographs of Pt/CNT samples prepared by conventional reflux heating method are shown in Fig. 7. These samples have a metal loading of 10 wt% and 30 wt% and are prepared with 10 vol% water content (Fig. 7a and b). When the metal loading was increased from 10 wt% to 30 wt%, more Pt nanoparticles were observed to be deposited on the outer wall of CNT. Fig. 8a and b shows the size distribution histograms, which correspond to the TEM images shown in Fig. 7a and b. Larger particles can be observed for 30 wt% Pt/CNT sample (Figs. 7b and 8b).

In addition, it is reasonable to assume that the larger diameter CNF attracts more Pt nanoparticles than the small diameter CNT. Fig. 9 shows TEM images of Pt/CNF samples with 30 wt% Pt loading prepared by the microwave irradiation method. At 10 vol% water content, it can be observed that uniform spherical Pt metal nanoclusters are homogeneously dispersed with a relatively small size distribution (Fig. 9a). As water content is increased to 30 vol% water (Fig. 9b), the particle size distribution becomes larger.

Fig. 10a and b shows the size distribution histograms, which correspond to the TEM images shown in Fig. 9a and b. It has been found that particle sizes determined by XRD are in good agreement with the values measured from TEM. Larger particles of more than 10 nm and some big Pt particle agglomerations can be observed under TEM. This may be attributed to uneven heating in the microwave and lack of

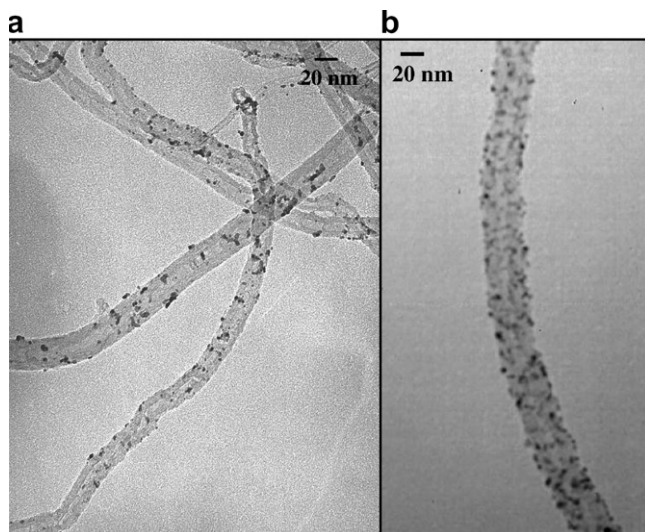


**Fig. 7 – High resolution TEM micrographs of catalyst from conventional heating (a) 10 wt% Pt/CNT (10 vol%) and (b) 30 wt% Pt/CNT (10 vol%).**

mixing of Pt precursor and nanocarbon support. Our experiments show that microwave irradiation dramatically simplifies the synthesis process and shortens the synthesis time. However, larger particle size and uneven dispersion are still observed via this process, especially for high metal loading catalysts (30 wt%). Modification of the microwave reactor and optimization of synthesis conditions may help reduce Pt particle size and improve Pt dispersion.

CV experiments were conducted in 0.5 M H<sub>2</sub>SO<sub>4</sub>. The Pt ECSA was calculated from the hydrogen desorption peak areas in the CV curves and was obtained from the following formula [30]:

$$\text{ECSA} = \frac{Q(\text{mC})}{0.22 \text{ mC/cm}^2}$$

where Q is the electric charge for hydrogen desorption and 0.22 mC/cm<sup>2</sup> is the hydrogen adsorption constant for polycrystalline Pt.

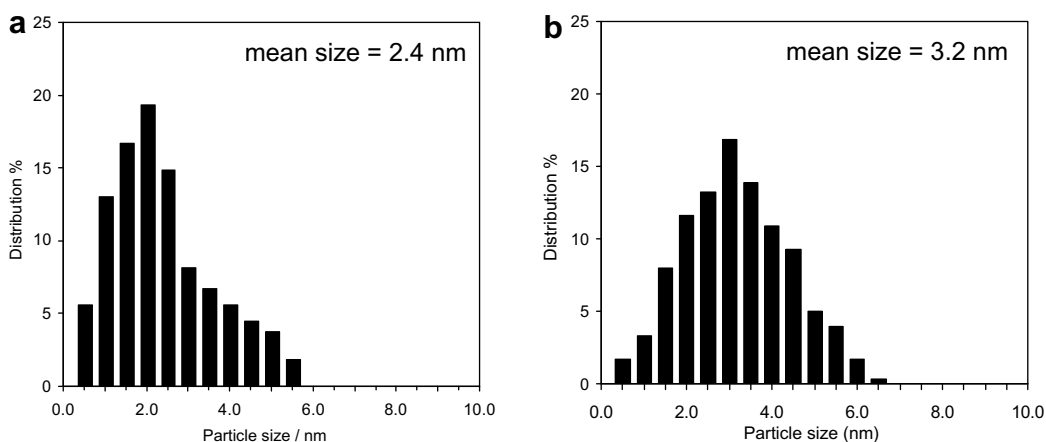


**Fig. 8 – Size distribution of catalyst from conventional reflux heating (a) 10 wt% Pt/CNT (10 vol%) and (b) 30 wt% Pt/CNT (10 vol%).**

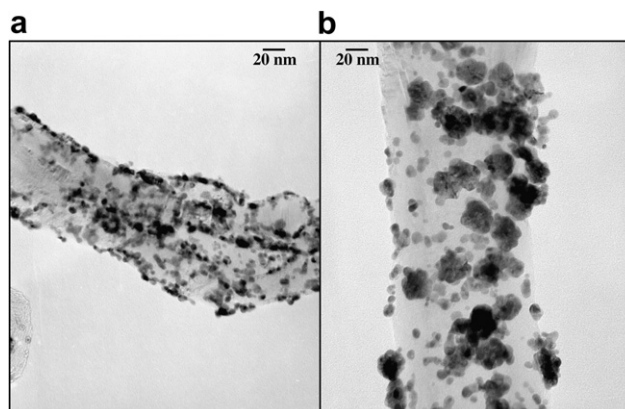


**Fig. 9 – High resolution TEM micrographs of catalyst from microwave irradiation (a) 30 wt% Pt/CNF (10 vol%) and (b) 30 wt% Pt/CNF (30 vol%).**

Fig. 11 shows the CV curves for various synthesized samples with different Pt particle size.

Table 1 summarizes the data for these nanocatalysts. The chemical surface area (CSA) of these catalysts was calculated using the following equation [30]:

$$\text{CSA} = \frac{6 \times 10^4}{\rho \times d}$$

where d is the mean Pt particle diameter in Å (from the XRD results) and ρ is the density of Pt metal (21.4 g/cm<sup>3</sup>). The Utilization efficiency can be calculated using [30]

$$\text{Utilization} = \frac{\text{ECSA}}{\text{CSA}}$$

Generally, catalysts with smaller particle size gave higher ECSA than those catalysts with larger particle size and distribution, e.g. CCNT10Pt10DI with a particle size of 2.3 nm has an ECSA of 68.7 m<sup>2</sup>/g, while MCNT30Pt30DI with a particle size of 5.1 nm has an ECSA of 30.1 m<sup>2</sup>/g. Under optimized synthesis condition, Pt/CNTs made via conventional techniques (CCNT10Pt10DI) gave the highest ECSA of 68.7 m<sup>2</sup>/g. CNTs made via microwave irradiation (MCNT10Pt10DI) showed

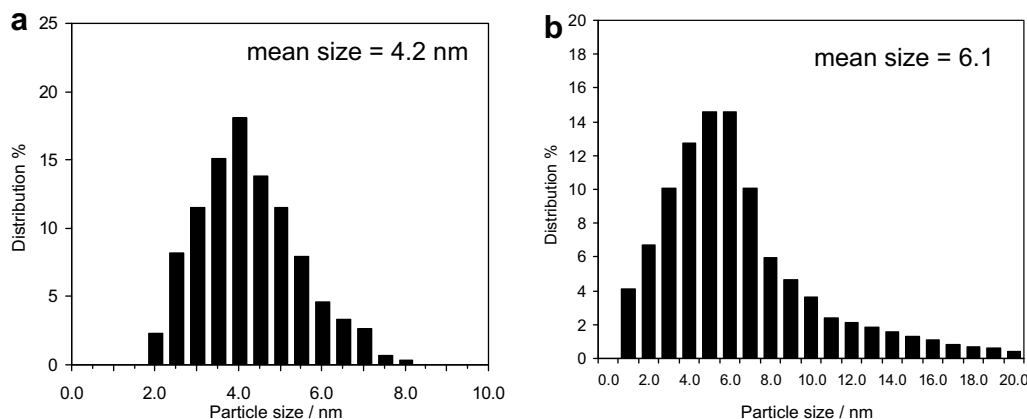


Fig. 10 – Size distribution of catalyst from microwave irradiation (a) 30 wt% Pt/CNF (10 vol%) and (b) 30 wt% Pt/CNF (30 vol%).

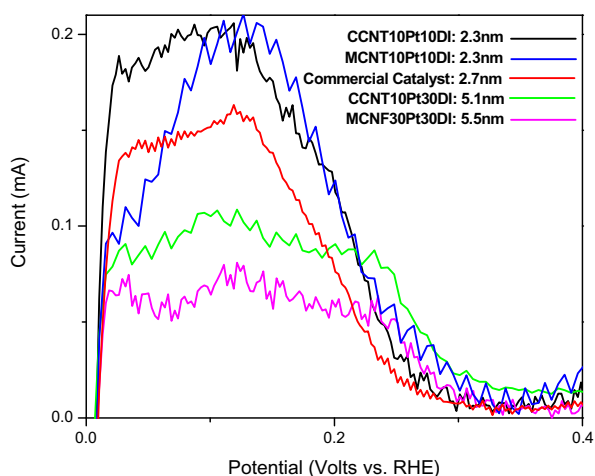


Fig. 11 – Hydrogen desorption peaks on cyclic voltammetry of different CNT/CNF supported Pt catalysts.

similar electrochemically active surface area (ECSA of 64.7 m<sup>2</sup>/g). The Pt utilization was in a range of 54–68%, with an exception of 47% for Pt/CNF (30 wt%, 30 vol%), this may

be due to a large particle size (5.5 nm) and a wider particle size distribution. It was reported that Pt utilization is around 75% for a commercial Pt/CB (20 wt%) catalyst [31]. All fabricated catalysts and their properties are shown in Table 1. There are two reasons that may explain slightly lower Pt utilization in our experiments: (1) use of sulfuric acid as electrolyte may result in HSO<sub>4</sub><sup>-</sup> adsorption on the Pt surface reducing its ECSA [32] and (2) using average particle sizes of Pt nanoparticles obtained from the XRD diffraction peak Pt(220) to calculate CSA of Pt, will generally result in smaller CSA than obtaining average Pt particle size from TEM [30]. Therefore, the Pt utilization is within a reasonable range. It is interesting to note that commercial (Pt/CB) catalyst has an ECSA of 50 m<sup>2</sup>/g and Pt utilization of 49%, which is lower than the CNT/CNF catalyst. In addition, there was no apparent trend of ECSA observed between different carbon nanomaterials (CNT and CNF). CNF supported catalyst gave comparable ECSA as the more expensive CNT, making it a more attractive candidate for future work in this area.

Altering water content during the synthesis can effectively control the particle size and moreover, the ECSA regardless of synthesis heating method and carbon support. In this work, we have found that the particle size and ECSA are inversely

Table 1 – The particle size, ECSA, CSA and Pt utilization for CNT and CNF supported Pt catalysts

Sample	Particle size (nm)	Q (mC)	ECSA (m <sup>2</sup> /g)	CSA (m <sup>2</sup> /g)	Utilization (%)
CCNT10PT10DI	2.3	0.76	68.7	123.4	55.7
CCNF10PT10DI	2.6	0.69	62.7	108.9	57.6
MCNT10PT10DI	2.3	0.71	64.8	120.7	53.7
MCNF10PT10DI	3.9	0.49	44.8	71.3	62.9
CCNT10PT30DI	5.1	0.39	35.4	55.2	64.2
CCNF10PT30DI	5.1	0.41	37.5	54.6	68.8
MCNT10PT30DI	4.7	0.42	38.1	59.3	64.2
MCNF10PT30DI	5.1	0.39	35.6	54.7	65.1
CCNT30PT10DI	3.2	0.53	48.4	87.5	55.3
MCNT30PT10DI	3.9	0.51	46.6	72.0	64.8
MCNF30PT10DI	4.2	0.46	42.0	67.5	62.2
MCNT30PT30DI	5.1	0.33	30.1	54.8	54.9
MCNF30PT30DI	5.5	0.26	24.0	51.4	46.8
Commercial catalyst	2.7	0.56	50.6	103.0	49.1

proportional for CNT/CNF supported Pt catalyst. It has been reported that there is an optimized Pt particle size around 3–5 nm for use in phosphoric acid fuel cells and ~2.6 nm for direct methanol fuel cells [33,8]. However, Watanabe et al. recently reported that ORR activities are particle size independent in a range of 1–5 nm [34]. Therefore, we reported a convenient way to control Pt particle size/ECSA to obtain the highest ORR activity. This work is underway in our lab.

#### 4. Conclusions

This study presents a systematical investigation to study the effects of two polyol based deposition techniques (conventional refluxing and microwave irradiation), synthesis parameters, such as water content, carbon support and Pt loading, on the average Pt particle size and ECSA. Uniformly dispersed Pt nanoparticles with narrow particle distribution were found to be deposited on CNT and CNF supports using polyol processing techniques. Microwave irradiation can significantly decrease the processing time and it does not considerably affect Pt particle size as compared to conventional refluxing, especially for high surface area CNT supported low Pt loading (10 wt%) catalyst. Modification of microwave process is needed to ensure small particle size as well as uniform dispersion of catalysts. Adjusting water content during synthesis effectively controlled particle size regardless of the heating method, carbon support and metal loading. Increasing the metal loading on a fixed surface area caused agglomeration. Larger diameter CNFs (100–200 nm) as compared to CNTs (20–40 nm) have less surface area and hence, larger particles are formed under same synthesis conditions. Optimum ECSA was observed during conventional heating for CNTs (68.7 m<sup>2</sup>/g) and during microwave irradiation for CNFs (64.8 m<sup>2</sup>/g), which exceeded the one obtained from commercial Pt/CB catalyst (50.6 m<sup>2</sup>/g).

#### Acknowledgments

The Authors would like to thank Christopher Dangler for BET analysis of carbon supports and Dr. Seiichiro Higashiya for TGA measurements.

#### REFERENCES

- [1] Vielstich W, Lamm A, Gasteiger H. Hand book of fuel cells. John Wiley & Sons Inc.; 2004.
- [2] Gasteiger HA, Panels JE, Yan SG. Dependence of PEM fuel cell performance on catalyst loading. *J Power Sources* 2004;127(1–2):162–71.
- [3] Nørskov JK, Rossmeisl J, Logadottir A, Lindqvist L, Kitchin JR, Bligaard T, et al. Origin of the overpotential for oxygen reduction at a fuel-cell cathode. *J Phys Chem B* 2004;108(46):17886–92.
- [4] Gasteiger HA, Kocha SS, Sompalli B, Wagner FT. Activity benchmarks and requirements for Pt, Pt-alloy, and non-Pt oxygen reduction catalysts for PEMFCs. *Appl Catal B – Environ* 2005;56(1–2):9–35.
- [5] Lee K, Zhang J, Wang H, Wilkinson DP. Progress in the synthesis of carbon nanotube- and nanofiber-supported Pt electrocatalysts for PEM fuel cell catalysis. *J Appl Electrochem* 2006;36(60):507–22.
- [6] Li W, Liang C, Zhou W, Qiu J, Zhou Z, Sun G, et al. Preparation and characterization of multiwalled carbon nanotube-supported platinum for cathode catalysts of direct methanol fuel cells. *J Phys Chem B* 2003;107(26):6292–9.
- [7] Matsumoto T, Komatsu T, Arai K, Yamazaki T, Kijima M, Shimizu H, et al. Reduction of Pt usage in fuel cell electrocatalysts with carbon nanotubes. *J Chem Commun* 2004:840–1.
- [8] Li W, Liang C, Zhou W, Qiu J, Zhou Z, Sun G, et al. Novel in situ synthesis of MWNTs-hydroxyapatite composites. *Carbon* 2004;42(2):423–6.
- [9] Yuan F, Ryu H. The synthesis, characterization, and performance of carbon nanotubes and carbon nanofibres with controlled size and morphology as a catalyst support material for a polymer electrolyte membrane fuel cell. *Nanotechnology* 2004;15(10):S596–602.
- [10] Wang X, Waje M, Yan Y. CNT-based electrodes with high efficiency for PEMFCs. *Electrochem Solid State Lett* 2005;8(1):A42–4.
- [11] Li W, Wang X, Chen Z, Waje M, Yan Y. Carbon nanotube film by filtration as cathode catalyst support for proton-exchange membrane fuel cell. *Langmuir* 2005;21(21):9386–9.
- [12] Waje MM, Wang X, Li W, Yan Y. Deposition of platinum nanoparticles on organic functionalized carbon nanotubes grown in situ on carbon paper for fuel cells. *Nanotechnology* 2005;16(7):S395–400.
- [13] Paschos O, Knupp SL, Pyoungcho C, Snyder J, Buelte S, Haldar P, et al. Carbon nanotube-supported platinum electrode for ORR in phosphoric acid solution – effect of PTFE content and annealing temperature. *Electrochem Solid State Lett* 2007;10(9):B147–9.
- [14] Wang X, Li W, Chen Z, Waje M, Yan Y. Durability investigation of carbon nanotube as catalyst support for proton exchange membrane fuel cell. *J Power Sources* 2006;158(1):154–9.
- [15] Yu W, Tu W, Liu H. Synthesis of nanoscale platinum colloids by microwave dielectric heating. *Langmuir* 1999;15(1):6–9.
- [16] Li X, Chen W, Zhao J, Xing W, Xu Z. Microwave polyol synthesis of Pt/CNTs catalysts: effects of pH on particle size and electrocatalytic activity for methanol electrooxidation. *Carbon* 2005;43(10):2168–74.
- [17] Raghuvver MS, Agrawal S, Bishop N, Ramanath G. Microwave-assisted single-step functionalization and in situ derivatization of carbon nanotubes with gold nanoparticles. *Chem Mater* 2006;18(6):1390–3.
- [18] Tian Z, Jiang S, Liang T, Shen P. Synthesis and characterization of platinum catalysts on multiwalled carbon nanotubes by intermittent microwave irradiation for fuel cell applications. *J Phys Chem B* 2006;110(11):5343–50.
- [19] Xing Y. Synthesis and electrochemical characterization of uniformly-dispersed high loading Pt nanoparticles on sonochemically-treated carbon nanotubes. *J Phys Chem B* 2004;108(50):19255–9.
- [20] Bock C, Paquet C, Couillard M, Botton GA, MacDougall BR. Size-selected synthesis of PtRu nano-catalysts: reaction and size control mechanism. *J Am Chem Soc* 2004;126(25):8028–37.
- [21] Ciacchi L, Pompe W, Vita A. Initial nucleation of platinum clusters after reduction of K<sub>2</sub>PtCl<sub>4</sub> in aqueous solution: a first principles study. *J Am Chem Soc* 2001;123(30):7371–80.
- [22] Li W, Bai Y, Zhang Y, Sun M, Cheng R, Xu X, et al. Effect of hydroxyl radical on the structure of multi-walled carbon nanotubes. *Synthetic Metals* 2005;155(3):509–15.
- [23] Misra A, Tyagi PK, Singh MK, Misra DS. FTIR studies of nitrogen doped carbon nanotubes. *Diamond Related Mater* 2006;15(2–3):385–8.



- [24] Wang Z, Liu Q, Hui H, Liu H, Chen Y, Yang M. Dispersing multi-walled carbon nanotubes with water-soluble block copolymers and their use as supports for metal nanoparticles. *Carbon* 2007;45(2):285–92.
- [25] Kordas K, Mustonen T, Tóth G, Jantunen H, Vajtai R, Ajayan PM. Inkjet printing of electrically conductive patterns of carbon nanotubes. *Small* 2006;2(8–9):1021–5.
- [26] Hull R, Li L, Xing Y, Chusuei C. Pt nanoparticle binding on functionalized multiwalled carbon nanotubes. *Chem Mater* 2006;18(7):1780–8.
- [27] Park ParkJongnam, An AnKwangjin, Hwang HwangYosun, Park ParkJe-Geun, Noh NohHan-Jin, Kim KimJae-Young, et al. Ultra-large-scale syntheses of monodisperse nanocrystals. *Nature Mater* 2004;3:891–5.
- [28] Zhou Z, Wang S, Zhou W, Wang G, Jiang L, Li W, et al. Novel synthesis of highly active Pt/C cathode electrocatalyst for direct methanol fuel cell. *Chem Commun* 2003;3:394–5.
- [29] Ralph TR, Hogarth MP. Catalysis for low temperature fuel cells. *Platinum Metal Rev* 2002;46(1):3–14.
- [30] Li W, Zhou W, Li H, Zhou Z, Zhou B, Sun G, et al. Nanostructured Pt-Fe/C as cathode catalyst in direct methanol fuel cell. *Electrochim Acta* 2004;49(7):1045–55.
- [31] Paulus UA, Wokaun A, Scherer G, Schmidt TJ, Stamenkovic V, Radmilovic V, et al. Oxygen reduction on carbon-supported Pt-Ni and Pt-Co alloy catalysts. *J Phys Chem B* 2002;106(16):4181–91.
- [32] Tamizhmani G, Dodelet JP, Guay DJ. Crystallite size effects of carbon-supported platinum on oxygen reduction in liquid acids. *Electrochem Soc* 1996;143(1):18–23.
- [33] Kinoshita K. Particle size effects for oxygen reduction on highly dispersed platinum in acid electrolytes. *J Electrochem Soc* 1990;137(3):845–8.
- [34] Yano H, Inukai J, Uchida H, Watanabe M, Babu PK, Kobayashi T, et al. Particle-size effect of nanoscale platinum catalysts in oxygen reduction reaction: an electrochemical and 195Pt EC-NMR study. *Phys Chem Chem Phys* 2006;8:4932–9.